# PHASE POLYMORPHISM OF $[M(OS(CH_3)_2)_6](ClO_4)_2$ (M=Mn(II) AND Zn(II) STUDIED BY TRANSMITTED LIGHT INTENSITY AND POLARIZED OPTICAL MICROSCOPY MEASUREMENTS

**E. Szostak[a]*, A. Migdał-Mikuli[a], J. Chruściel[b] and A. Rudzki[b]**

**Keywords:** hexakis(dimethylsulphoxide)manganese(II) tetraoxochlorate(VII); hexakis(dimethylsulphoxide)zinc tetraoxochlorate(VII); phase transitions; melting points; transmitted light intensity; polarized optical microscopy.

The transmitted light intensity (TLI) and polarized optical microscopy (POM) measurements of $[Mn(OS(CH_3)_2)_6](ClO_4)_2$ and $[Zn(OS(CH_3)_2)_6](ClO_4)_2$, as a function of temperature, showed that only some of the phase transitions discovered earlier for these compounds by the differential scanning calorimetry were now observed as anomalies on the TLI curves and as different textures in POM pictures. Above-mentioned methods indicated that discovered phases of both compounds were the crystalline phases with different orientational dynamical disorder. Additionally, it was confirmed that these both compounds melt at 488 and 465 K, respectively.

*Corresponding Authors*
ax: +48 12 664 0515
E-Mail: szostak@chemia.uj.edu.pl
[a] Faculty of Chemistry, Jagiellonian University, ul. Ingardena 3, 30–060 Kraków, Poland,
[b] Faculty of Sciences, Siedlce University of Natural Sciences and Humanities, ul. 3 Maja 54, 08-110 Siedlce, Poland,

## Introduction

Physicochemical properties of coordination compounds of $[M(OS(CH_3)_2)_6]X_2$, type containing DMSO ligands have been the subject of research studies for a long time.[1-10] These studies have revealed very rich and interesting phase polymorphism of these substances. The number and type of the phase transitions depends on the chemical nature of the cation and anion, as well as on so-called "thermal history" of the sample. In this article, we will present some new results obtained for $[Mn(OS(CH_3)_2)_6](ClO_4)_2$ and $[Zn(OS(CH_3)_2)_6](ClO_4)_2$.

At room temperature $[Mn(OS(CH_3)_2)_6](ClO_4)_2$ crystallizes in the orthorhombic system (Fdd2 space group, No. = 43) and $[Zn(OS(CH_3)_2)_6](ClO_4)_2$ in the trigonal system ($P3_1c$ space group, No. = 159), with eight and two molecules in an elementary unit cell, respectively.[11,12] They are isostructural with $[Cd(OS(CH_3)_2)_6](ClO_4)_2$ and $[Ni(OS(CH_3)_2)_6](ClO_4)_2$ compounds, respectively.[1,6] We have recently investigated the polymorphism of the above mentioned compounds ($[M(DMSO)_6](ClO_4)_2$, where M = Cd, Ni Mn, Zn) using differential scanning calorimetry (DSC) and have found that they have at least four higher temperature polymorph phases.[1,3,4,6] Some of these phases can be very easily overcooled to form metastable states. The orthorhombic compounds show an additional phase transition below room temperature. At this phase transition the crystal structure of these compounds changes from orthorhombic to monoclinic. Compounds which crystallize in the trigonal system do not show any low temperature phase transitions.

In this work transmitted light intensity (TLI) and polarized optical microscopy (POM) measurements were performed to follow the nature (phase transition or changes in molecular dynamics) of transitions detected in our earlier DSC experiments in the temperature range of 273–473 K.

## EXPERIMENTAL

### Sample Preparation

All measured samples were prepared and their chemical composition were determined by the methods described previously.[3,4,13] The chemical identity and purity of the examined compounds have been also confirmed by Fourier transform Raman scattering (FT-RS) and infrared absorption (FT-IR) spectra and additionally by thermal analysis methods (TG + QMS and SDTA).[3,4]

### Transmitted Light Intensity and Polarized Optical Microscopy measurements

The TLI measurements were made using Dresden Analitik polarizing microscope with a home-made set-up, equipped with Burr-Brown photodiode OPT101 (source of light, polarizing microscope, detector - photodiode and recorder), the heating stage and the temperature controller were the same as in POM measurements.

The POM measurements were carried out using Nicon polarizing microscope Eclipse E200 equipped with Linkam heating stage THMSE 600 and temperature controller TMS 93 and digital camera DG-01 (CHUGAI BOYEKI).

## RESULTS AND DISCUSSION

### $[Mn(OS(CH_3)_2)_6](ClO_4)_2$

The thermodynamic parameters obtained for phase transitions of $[Mn(DMSO)_6](ClO_4)_2$ by our earlier DSC measurements and the schematic representation of the Gibbs free energy (G)-temperature relationship are given in Table and Figure 1, respectively.

**Table 1.** Thermodynamics parameters of the phase transitions detected in $[Mn(OS(CH_3)_2)_6](ClO_4)_2$.[3]

| | Heating | | | Cooling | | |
|---|---|---|---|---|---|---|
| | $\Delta T \pm S_{\Delta T}$, K | $\Delta H \pm S_{\Delta H}$, kJ·mol$^{-1}$ | $\Delta S \pm S_{\Delta S}$, J·mol$^{-1}$·K$^{-1}$ | $\Delta T \pm S_{\Delta T}$, K | $\Delta H \pm S_{\Delta H}$, kJ·mol$^{-1}$ | $\Delta S \pm S_{\Delta S}$, J·mol$^{-1}$·K$^{-1}$ |
| $T_m$ | 488 ± 3 | 37.83 ± 1.30 | 184.5 ± 1.7 | – | – | – |
| $T_{c1}$ | 379 ± 1 | 3.43 ± 0.40 | 9.1 ± 1.1 | – | – | – |
| $T_{c2}$ | 376 ± 2 | 4.44 ± 0.45 | 11.8 ± 1.2 | 370 ± 2 | 5.27 ± 0.4 | 14.2 ± 1.2 |
| $T_{c3}$ | 365 ± 3 | 27.11 ± 1.24 | 74.3 ± 2.9 | – | – | – |
| $T_{c4}$ | 322 ± 3 | 16.60 ± 0.62 | 51.6 ± 1.8 | 315 ± 4 | 16.4 ± 0.8 | 52.0 ± 2.3 |
| $T_{c5}$ | 225 ± 1 | 0.88 ± 0.11 | 2.0 ± 0.3 | 223 ± 1 | 0.8 ± 0.2 | 1.9 ± 0.5 |

The sample without "thermal history" contains the crystalline phase called Cr 1. The TLI measurements were started by heating of this sample from room temperature (RT) up to 393 K. Upon heating the sample a phase transition was occurred when the Cr1 phase was transformed into the intermediate Rot. 2 phase at $T_{C3}$ = 365 K (see Figure 2 and compare it with Figure 1). Due to this transition, a distinct anomaly on TLI curve was recorded, which could be related to significant decreasing of the transmitted light intensity.

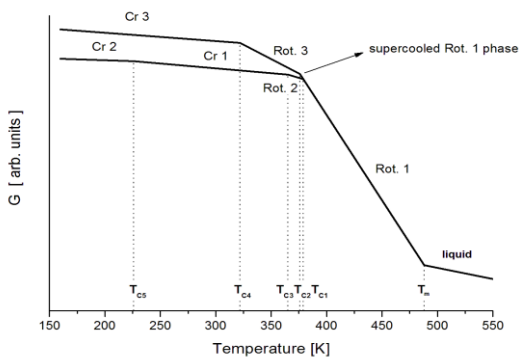


**Figure 1.** Scheme of the temperature dependence of free enthalpy $G$ for $[Mn(OS(CH_3)_2)_6](ClO_4)_2$.

During further heating of the sample, the phase Rot. 2 was transformed into the high temperature Rot. 1 phase at $T_{C1}$ = 379 K, which was manifested in a very small anomaly on TLI curve.

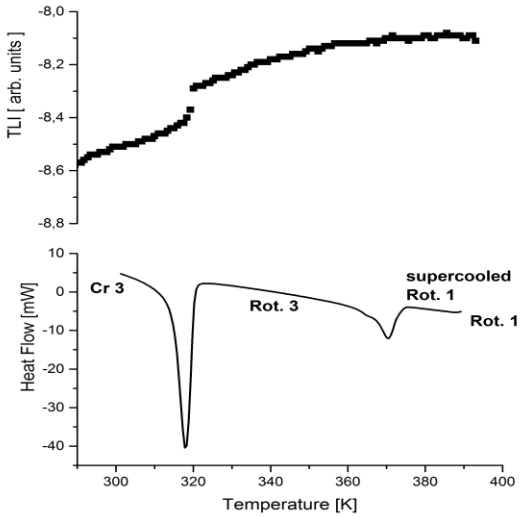


**Figure 3.** Differential scanning calorimetry and transmitted light intensity curves obtained during cooling $[Mn(OS(CH_3)_2)_6](ClO_4)_2$ from 393 to 298 K.

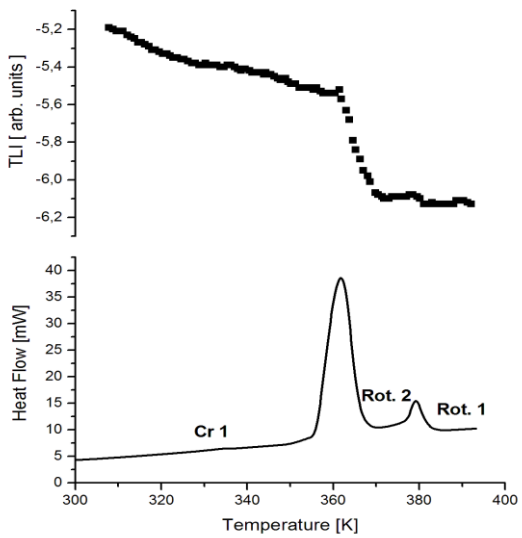


**Figure 2.** Differential scanning calorimetry and transmitted light intensity curves obtained during heating $[Mn(OS(CH_3)_2)_6](ClO_4)_2$ from 300 to 393 K.

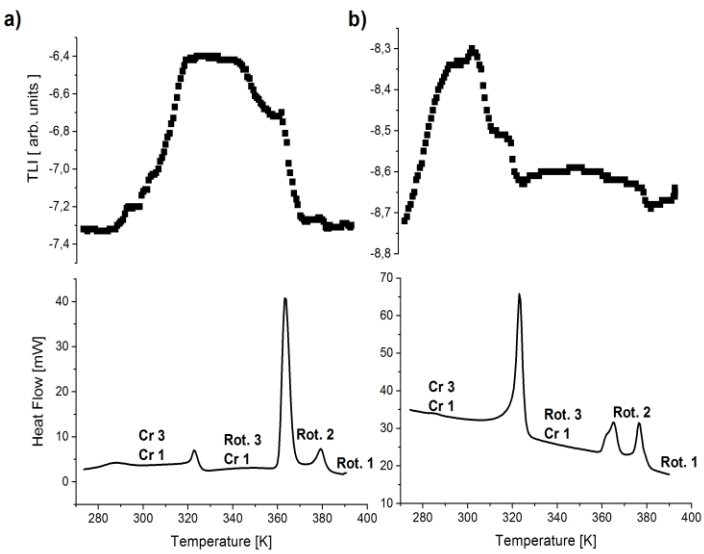


**Figure 4.** Differential scanning calorimetry and transmitted light intensity curves obtained during heating $[Mn(OS(CH_3)_2)_6](ClO_4)_2$ from 270 to 393 K.

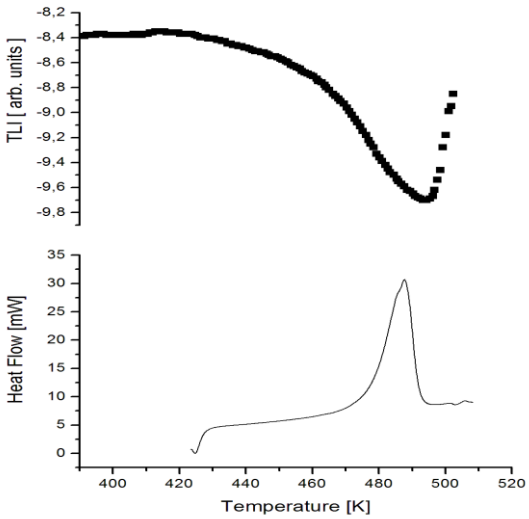


**Figure 5.** Differential scanning calorimetry (DSC) and transmitted light intensity curves obtained during heating $[Mn(OS(CH_3)_2)_6](ClO_4)_2$ from 393 to 510 K.

Cooling the sample Rot. 1 phase from 393 K to 298 K, results in a phase that is slightly supercooled. The supercooled Rot. 1 phase undergoes a phase transition at $T_{C2}$ = 370 K into the metastable phase Rot. 3. However, this transition does not change the transmitted light intensity. Being further cooled down, the Rot. 3 phase goes into the Cr 3 phase at $T_{C4}$ = 315 K (see Figure 3 and compare it with Figure 1).

The phase transition at $T_{C4}$ was observed on the TLI curve as an anomaly connected to an insignificant decrease of the transmitted light intensity. It is known from our previous DSC measurements that when the heating speed is high the phase transition from the supercooled Rot. 1 phase to the Rot. 3 phase (at $T_{C2}$) and the transition from the Rot. 3 phase into the Cr 3 phase (at $T_{C4}$) are reversible transitions,[3] however, when the heating is slow, the phases Rot. 3 and Cr 3 convert into stable phase Cr 1. It is clearly visible in Figure 4 a and b, which show the TLI curves, recorded during heating the sample in a temperature range 273-393 K with a rate of 2 K min$^{-1}$. The observed initially increase of the transmitted light intensity on TLI curve is probably attributed to a relatively slow spontaneous conversion of the metastable Cr 3 phase into the stable Cr 1 phase. This process might be taken as an analogue of a new phase crystallisation.[14] On further heating, the rest of the Cr 3 phase undergoes a phase transitions into the phase Rot. 3 and supercooled Rot 1. At the end, stable phase Cr 1 undergoes a phase transition into the stable Rot. 1 phase at the temperature $T_{C1}$ = 379 K. The DSC curves presented in Figure 4, below the TLI curves, show the possible ways of spontaneous conversion of these polymorphs into the stable phase Cr 1.

Heating up the hermetically closed sample above the $T_{C1}$ temperature, the sample melts at $T_m$ = 488 K. As it can be seen in Figure 5, the TLI curve unambiguously shows the anomaly resulting from the melting process. Table 2 indicates the phase transitions registered as anomalies on TLI curves associated with a change of the sample texture.

The textures of $[Mn(OS(CH_3)_2)_6](ClO_4)_2$ at different phases were recorded using POM in a function of temperature and presented in Figure 6. Measurements were conducted with the scanning rate of 10 K min$^{-1}$ in four steps. At first, the sample was cooled down from 293 to 203 K. In two next steps, the sample was heated up to 393 K and then cooled down to 273 K. In the last step the sample was heated up to 486 K. As can be seen in Figure 6, the greatest differences between POM textures were registered for solid Cr 1, Rot. 2 and Rot. 1 phases (Figures 6b-6d)). Moreover some small changes in the brightness and sharpness of POM textures of Rot 3 and Cr 3, and Cr 2 and Cr 1 phases were also observed (Figures 6e, 6f and 6a, 6b).

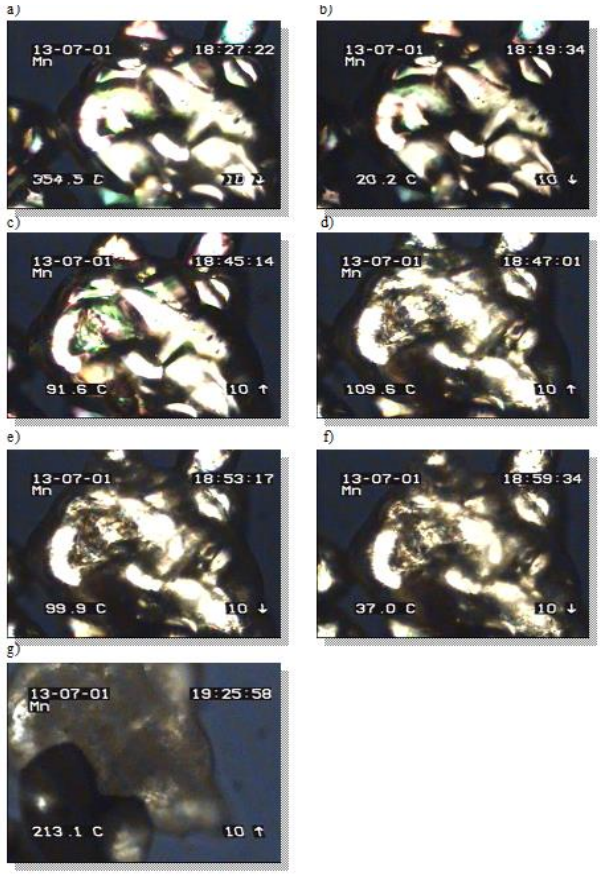


**Figure 6.** $[Mn(OS(CH_3)_2)_6](ClO_4)_2$ crystal images obtained using POM at the temperature: a) 218 K – phase Cr 2, b) 293 K – phase Cr 1, c) 365 K – phase Rot. 2, d) 383 K – phase Rot. 1, e) 373 K – phase Rot. 3, f) 310 K – phase Cr 3 and g) 486 K – liquid.

Heating of the sample above 393 K causes melting of Rot. 1 phase at ca. 486 K. This transition was registered in the last step of POM measurement. The view of liquid form of $[Mn(OS(CH_3)_2)_6](ClO_4)_2$ compound was presented in Figure 6g.

**Table 2.** Phase transitions of $[Mn(DMSO)_6](ClO_4)_2$ detected by TLI method

| | Heating | Cooling |
|---|---|---|
| $T_C$ | | |
| $T_m$ | + | – |
| $T_{C1}$ | + | – |
| $T_{C2}$ | – | – |
| $T_{C3}$ | + | – |
| $T_{C4}$ | + | + |
| $T_{C5}$ | – | – |

The phase transitions observed by both DSC and TLI methods are denoted as "+". The phase transitions which were observed by DSC but could not be observed by TLI method are denoted as " – ".

**Table 3.** Thermodynamics parameters of the phase transitions detected in $[Mn(OS(CH_3)_2)_6](ClO_4)_2$.[3]

| | Heating | | | Cooling | | |
|---|---|---|---|---|---|---|
| | $\Delta T \pm S_{\Delta T}$, K | $\Delta H \pm S_{\Delta H}$, kJ·mol$^{-1}$ | $\Delta S \pm S_{\Delta S}$, J·mol$^{-1}$·K$^{-1}$ | $\Delta T \pm S_{\Delta T}$, K | $\Delta H \pm S_{\Delta H}$, kJ·mol$^{-1}$ | $\Delta S \pm S_{\Delta S}$, J·mol$^{-1}$·K$^{-1}$ |
| $Tm_2$ | 456 ± 3 | 21.42 ± 0.82 | 47.0 ± 2.1 | – | – | – |
| $Tm_1$ | 389 ± 2 | 7.63 ± 0.23 | 19.6 ± 0.6 | 386 ± 1 | 7.48 ± 0.14 | 19.4 ± 0.4 |
| $Tc_1$ | 355 ± 1 | 25.33 ± 0.69 | 71.4 ± 1.9 | – | – | – |
| $Tc_2$ | 341 ± 1 | 2.37 ± 0.30 | 7.0 ± 0.9 | – | – | – |
| $Tc_3$ | 315 ± 1 | 21.31 ± 3.15 | 67.7 ± 10.3 | 309 ± 1 | 18.80 ± 5.62 | 60.8 ± 18.2 |

**$[Zn(OS(CH_3)_2)_6](ClO_4)_2$**

The thermodynamic parameters obtained for phase transitions of $[Zn(DMSO)_6](ClO_4)_2$ based on our earlier DSC measurements and the schematic representation of the Gibbs free energy (*G*)-temperature relationship are given in Table and Fig. 1, respectively.[4]

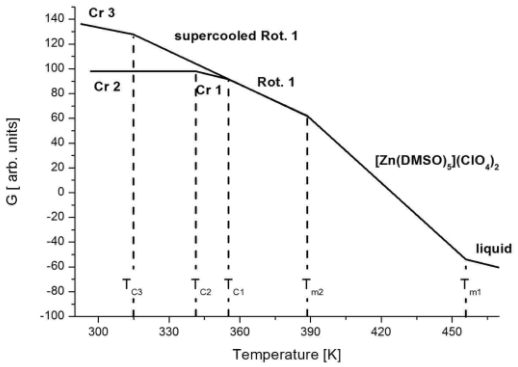


**Figure 7.** Scheme of the temperature dependence of free enthalpy *G* for $[Zn(OS(CH_3)_2)_6](ClO_4)_2$.

The measurements were started by heating the sample from room temperature (RT) to 373 K. While heating the sample, being initially in the Cr 2 phase, the phase transition into intermediate phase which was named Cr 1 can be observed on DSC curve at $T_{C2}$ = 341 K (see Fig. 8). This transition was not registered on the TLI curve what suggests that it is no connected with changing of the sample texture. Phase Cr 1 next transforms at $T_{C1}$ = 355 K into the high temperature phase, named Rot. 1, that is manifested as a big anomaly on the DSC curve and small anomaly on the TLI curve.

Cooling of the sample being in Rot. 1 phase may happen in two different ways. In the first case the Rot. 1 phase transforms into the Cr 2 phase which next transforms into the Cr 1 phase. In the second case phase transition occurs between the supercooled Rot. 1 and metastable Cr 3 phase. As seen by the DSC measurements usually during this process metastable Cr 3 phase transforms exothermically into the stable Cr 1 phase (see the DSC curve in Figure 9).

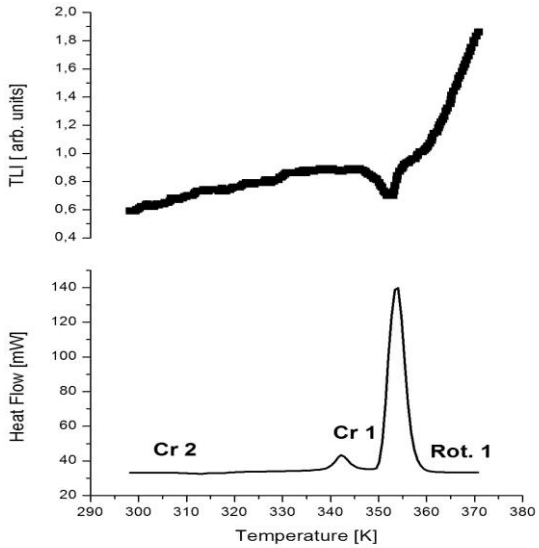


**Figure 8.** DSC and TLI curves obtained during heating $[Zn(OS(CH_3)_2)_6](ClO_4)_2$ from 298 to 373 K.

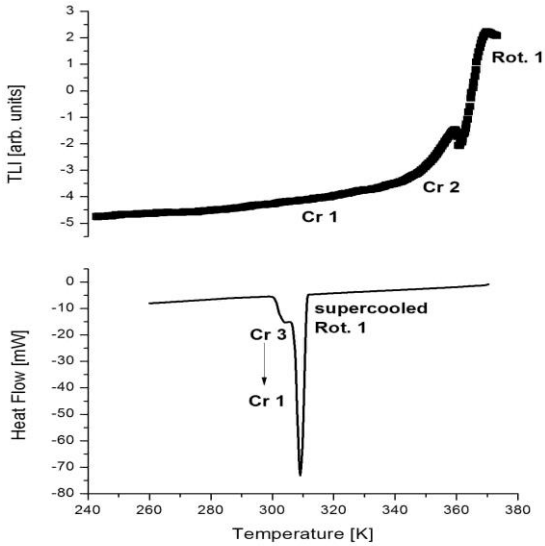


**Figure 9.** DSC and TLI curves obtained during cooling $[Zn(OS(CH_3)_2)_6](ClO_4)_2$ from 373 to 240 K.

Phase transitions between phases: Rot. 1 ↔ Cr 2 ↔ Cr 1 were not recorded on the DSC curve but are clearly visible on the TLI curve (see the TLI curve in Fig. 9).

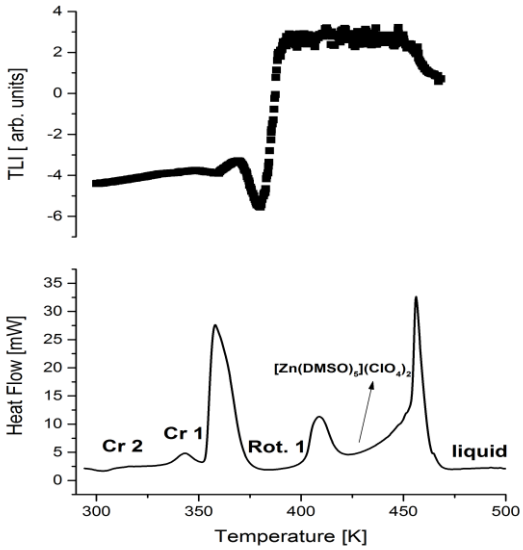


**Figure 10.** DSC and TLI curves obtained during heating $[Zn(OS(CH_3)_2)_6](ClO_4)_2$ from 298 to 500 K.

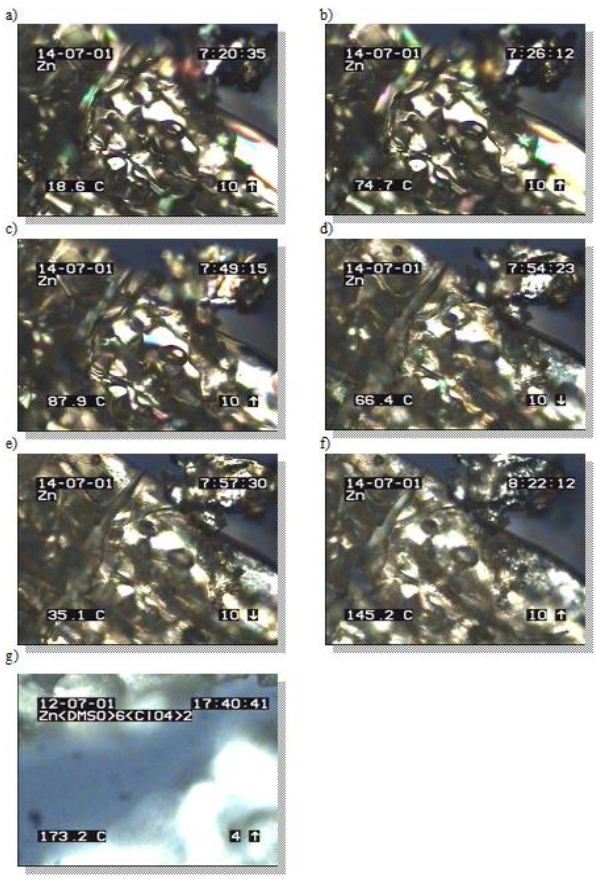

**Figure 11.** $[Zn(OS(CH_3)_2)_6](ClO_4)_2$ crystal images obtained using thermal microscope at the temperature: a) 292 K – phase Cr 2, b) 348 K – phase Cr 1, c) 361 K – phase Rot. 1, d) 339 K – supercooled phase Rot. 1, e) 308 K – phase Cr 3, f) 418 K – $[Zn(OS(CH_3)_2)_5](ClO_4)_2$ crystal and g) 446 K – liquid.

Second heating of the sample from 300 K to 373 K gives similar results as registered before both on DSC and TLI curves. During further heating above the $T_{C1}$ temperature, hermetically closed sample partially melts at $T_{m2}$ = 389 K, and then it completely melts at $T_{m1}$ = 465 K. All mentioned above phase transitions are connected with the change of the intensity of the transmitted light (see Figure 10).

To observe of all the phases occurring in $[Zn(OS(CH_3)_2)_6](ClO_4)_2$, the POM measurements at different temperature were conducted in five steps. In the first step, the sample was heated from 273 to 348 K and then cooled down from 348 to 243 K. In two next steps, the sample was heated in the temperature range of 243-375 K and cooled in the range of 375-243 K. In the last step the sample was heated from 243 up to 453 K.

**Table 4.** Phase transitions of $[Zn(DMSO)_6](ClO_4)_2$ detected by TLI method

| | Heating | Cooling |
|---|---|---|
| $T_C$ | | |
| $T_{m1}$ | + | – |
| $T_{m2}$ | + | – |
| $T_{C1}$ | + | +/- |
| $T_{C2}$ | – | – |
| $T_{C3}$ | – | – |

The phase transitions observed by both DSC and TLI methods are denoted as "+". The phase transitions which were observed by DSC but could not be observed by TLI method are denoted as "–". The "+/-" this transition was only observed by TLI method.

Figure 11 presents the POM textures of all phases which were detected earlier by DSC method[4]. As can be seen in this figure the most significant differences between POM textures were obtained for the phases: Cr 1 and Rot 1 (Figures 6(b, c), Rot 1 and $[Zn(OS(CH_3)_2)_5](ClO_4)_2$ crystal (Figures 6(c, f), $[Zn(OS(CH_3)_2)_5](ClO_4)_2$ crystal and liquid (Figures 6(f, g). Table 4 indicate which of the phase transitions registered as anomalies on TLI curves are associated with a change of the sample texture.

## CONCLUSIONS

1. The TLI measurements performed in a function of temperature showed that not all of the phase transitions observed earlier by the DSC method for $[Mn(OS(CH_3)_2)_6](ClO_4)_2$ and $[Zn(OS(CH_3)_2)_6](ClO_4)_2$ were observed as anomalies on the TLI curves. These anomalies can be associated with a change of the sample texture.

2. The POM observations performed in a function of temperature indicated only small differences between some pictures confirmed that all phases of $[Mn(OS(CH_3)_2)_6](ClO_4)_2$ and $[Zn(OS(CH_3)_2)_6](ClO_4)_2$, investigated earlier by the DSC method, are the crystalline phases, and that these crystals melt at ca. 488 and 465 K, respectively.

3. DSC, TLI and POM measurements indicated that discovered phases of both compounds were the crystalline phases with different orientational dynamical disorder.

## References

[1]Migdał-Mikuli, A., Mikuli, E., Szostak, E., Serwońska J., *Z. Naturforsch.* **2003,** *58a*, 341-345.

[2]Migdał-Mikuli, A., Szostak, E., *Thermochim. Acta*. **2005,** *426*, 191-198.

[3]Migdał-Mikuli, A., Szostak, E., *Z. Naturforsch*. **2005,** 60a, 289-295.

[4]Migdał-Mikuli, A., Szostak, E., *Thermochim. Acta*. **2006**, *444*, 195-200.

[5]Migdał-Mikuli, A., Skoczylas, Ł., Szostak, E.., *Z. Naturforsch.* **2006**, 61a, 180-188.

[6]Migdał-Mikuli, A., Szostak, E., *Z. Naturforsch*. **2007**, *62a*, 67-74.

[7]Migdał-Mikuli, A., Szostak, E., Drużbicki, K., Dołęga, D., *J. Therm. Anal. Calor*. **2008,** 93, 853-856.

[8]Migdał-Mikuli, A., Skoczylas, Ł., Szostak, E., *J. Coord. Chem.* **2008**, *61*, 2197-2206.

[9]Szostak, E., Migdał-Mikuli, A., *J. Therm. Anal. Calor*. **2010** 101, 601-606.

[10]Migdał-Mikuli, A., Szostak, E., Bernard, P., *J. Therm. Anal. Calor*. **2014,** *115*, 443-449.

[11]Migdał-Mikuli, A., Szostak, E., Nitek, W., *Acta Cryst. E*. **2006,** *62*, m2581-m2582.

[12]Persson, I., *Acta Chem. Scand*. **1982,** *36a*, 7-13.

[13]Cotton, F. A., Francis, R., *J. Am. Chem. Soc.* **1960,** *82(12)*, 2986-2991.

[14]Mnyukh, Y., *Fundamentals of Solid-State Phase Transitions, Ferromagnetism and Ferroelectricity*. Bloomington: 1st Books Library; **2001**.

Received: 09.10.2015.
Accepted: 06.11.2015.